is a useful tool for assessing whether or not label/duplex interactions are present and whether or not label attachment has significantly affected the ability of the complementary strands to hybridize. The combination of thermodynamic measurements and steady-state and time-resolved emission studies has been shown to provide a consistent and complementary view of label/label and label/duplex interactions.

The next step is to refine the molecular design strategy to optimize label/label interactions. An important improvement would be the construction of more rigid linker arms to minimize label/duplex association. This could be done by introducing either a six-membered ring like piperazine or an alkyne into the attachment modification. For the former case, ethylenediamine could be replaced by piperazine in the synthesis of the modified thymidine reported here. For the latter case, linker arms with a terminal primary amine could be derived from propargylamine.[31] Another design improvement would involve attaching labels at internucleotide phosphate sites. Such labeling is less likely to interfere with base pairing than is base labeling, yet flexibility in label location is preserved. Phosphate labeling has been used at terminal sites by several groups to prepare singly labeled duplexes.[5,6] Finally, a good molecular design would employ hydrophilic labels whenever possible to minimize further label/duplex association. When these steps are taken, it will be possible to prepare DNA-based macromolecules with specifically located molecular subunits. Some fundamental processes that these subunits can be arranged to carry out are energy, electron, and proton translocations.

Acknowledgment. The technical assistance of Raymond J. Carroll and Daniel L. Stockwell is gratefully appreciated. We thank Dr. Michael R. Wasielewski, Argonne National Laboratory, and Prof. Robert L. Letsinger, Northwestern University, for many helpful discussions. We particularly wish to thank Prof. Graham R. Fleming, University of Chicago, for helpful discussions and for providing facilities for emission lifetime measurements.

Registry No. GCACTCAG, 121329-89-3; CTGAGTGC, 121808-78-4; GCAC(T*)CAG, 121351-63-1; CTGAG(T*)GC, 121808-81-9; GCACTCAG + CTGAGTGC, 121844-89-1; GCAC(T*)CAG + CTGAGTGC, 121808-84-2; GCACTCAG + CTGAG(T*)GC, 121844-90-4; GCAC(T*)CAG + CTGAG(T*)GC, 121808-88-6; T*-pyrenebutyrate, 121808-79-5; T*-pyrenebutyrate + CTGAGTGC, 121808-85-3; T*-pyrenesulfonate, 121808-80-8; T*-pyrenesulfonate + CTGAGTGC, 121808-86-4; T*-anthraquinone, 121808-82-0; GCACTCAG + T*-anthraquinone, 121808-87-5; 1-pyrenebutanoic acid, 3443-45-6; sodium 1-pyrenesulfonate, 59323-54-5; *N*-(1-pyrenesulfonyl)-ethylenediamine, 121808-83-1.

(31) Prober, J. M.; Trainor, G. L.; Dam, R. J.; Hobbs, F. W.; Robertson, C. W.; Zagursky, R. J.; Cocuzza, A. J.; Jensen, M. A.; Baumeister, K. *Science* **1987**, *238*, 336.

Preparation and Characterization of an Aflatoxin B_1 Adduct with the Oligodeoxynucleotide $d(ATCGAT)_2$

S. Gopalakrishnan, Michael P. Stone,* and Thomas M. Harris*

Contribution from the Department of Chemistry and Center in Molecular Toxicology, Vanderbilt University, Nashville, Tennessee 37235. *Received February 23, 1989*

Abstract: Preparation of a double-stranded aflatoxin B_1–oligodeoxynucleotide adduct by direct addition of aflatoxin B_1 8,9-epoxide to $d(ATCGAT)_2$ is described. Reaction occurred rapidly at 5 °C to give a high yield of adduct. The reaction reached a limiting stoichiometry of 1:1 aflatoxin B_1 to $d(ATCGAT)_2$. The major product, which exhibited UV absorbance at 360 nm, was identified as 8,9-dihydro-8-{N^7-guanyl[d(ATCGAT)]}-9-hydroxyaflatoxin B_1·d(ATCGAT). Reversed-phase HPLC yielded equimolar quantities of unmodified d(ATCGAT) and 8,9-dihydro-8-{N^7-guanyl[d(ATCGAT)]}-9-hydroxyaflatoxin B_1. Acid hydrolysis followed by reversed-phase HPLC yielded 8,9-dihydro-8-N^7-guanyl-9-hydroxyaflatoxin B_1 [Essigmann, J. M.; Croy, R. G.; Nadzan, A. M.; Busby, W. F., Jr.; Reinhold, V. N.; Büchi, G.; Wogan, G. N. *Proc. Natl. Acad. Sci. U.S.A.* **1977**, *74*, 1870–1874. Lin, J. K.; Miller, J. A.; Miller, E. C. *Cancer Res.* **1977**, *37*, 4430–4438]. Gentle heating at pH 8 and subsequent acid hydrolysis gave products consistent with formation of formamidopyrimidine (FAPY) aflatoxin B_1 derivatives. Circular dichroism measurements showed negative ellipticity at 360 nm and an increase in positive ellipticity at 260 nm as compared to unmodified $d(ATCGAT)_2$. UV melting curves demonstrated that adduct formation increased duplex stability. Spontaneous depurination of the modified duplex was observed but was sufficiently slow at 5 °C and neutral pH to obtain NMR spectra. ^{1}H NMR spectra exhibited a doubling of oligodeoxynucleotide resonances upon adduct formation due to loss of strand symmetry; strand exchange between modified and unmodified oligodeoxynucleotide duplexes was slow on the NMR time scale. Adduct formation resulted in increased shielding for aflatoxin protons. The C^8 proton of the modified guanine was not observed in the ^{1}H NMR spectrum in D_2O, but an additional signal tentatively assigned as that proton was observed at 9.75 ppm in the spectrum in H_2O. This signal was not observed after mild basic hydrolysis of the duplex cationic adduct. Six hydrogen-bonded NH resonances were observed between 12 and 14 ppm. ^{31}P NMR showed a doubling of resonances and one signal shifted downfield at least 1 ppm. A structure for the adduct is proposed in which the aflatoxin moiety is intercalated above the 5′ face of the modified guanine.

Aflatoxin B_1 (AFB1, **1**) is among the most potent environmental mutagens.[1] It is an established animal carcinogen and is implicated as a human carcinogen. Genotoxicity requires oxidative activation involving the 8,9 double bond in the terminal furan moiety. Although the product of this oxidation, putatively epoxide **2**, has never been detected in biological systems, its existence has been postulated on the basis of in situ reaction of microsomally activated **1** with DNA followed by hydrolysis to give products consistent with structure **2** for the reactive electrophile.[2] Fur-

(1) For review see: (a) Busby, W. F., Jr.; Wogan, G. N. In *Chemical Carcinogens*, 2nd ed.; Searle, C., Ed.; ACS Monograph Series 182; American Chemical Society: Washington, DC, 1984; pp 945–1136. (b) Essigmann, J. M.; Green, C. L.; Croy, R. G.; Fowler, K. W.; Büchi, G.; Wogan, G. N. *Cold Spring Harbor Symp. Quant. Biol.* **1983**, *47*, 327–337. (c) Hsieh, D. P. H.; Wong, J. J. In *Biologically Active Intermediates*; Snyder, et al., Eds.; Plenum: New York, 1982; pp 847–863. (d) Garner, R. C. *Br. Med. Bull.* **1980**, *36*, 47–52.

(2) (a) Essigmann, J. M.; Croy, R. G.; Nadzan, A. M.; Busby, W. F., Jr.; Reinhold, V. N.; Büchi, G.; Wogan, G. N. *Proc. Natl. Acad. Sci. U.S.A.* **1977**, *74*, 1870–1874. (b) Lin, J. K.; Miller, J. A.; Miller, E. C. *Cancer Res.* **1977**, *37*, 4430–4438. (c) Croy, R. G.; Essigmann, J. M.; Reinhold, V. M.; Wogan, G. N. *Proc. Natl. Acad. Sci. U.S.A.* **1978**, *75*, 1745–1749. (d) Garner, R. C.; Miller, E. C.; Miller, J. A. *Cancer Res.* **1972**, *32*, 2058–2066.

0002-7863/89/1511-7232$01.50/0

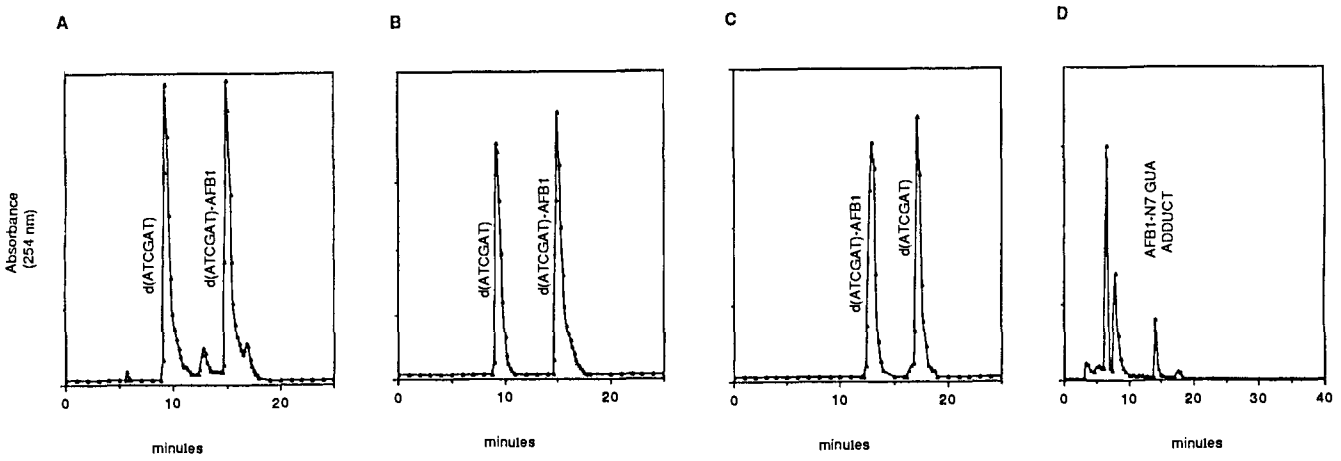

Figure 1. HPLC analysis of AFB1 adducts with d(ATCGAT)$_2$: (A) C_{18} chromatography of the crude reaction mixture after addition of epoxide **2** to d(ATCGAT)$_2$ yields two principal components, which correspond to unmodified d(ATCGAT) and single-strand adduct **5**; (B) C_{18} chromatography of adduct **3** after purification to remove minor impurities present in the crude reaction mixture; (C) strong anion-exchange chromatography of adduct **3** demonstrating that modified strand **5** elutes before the unmodified strand; (D) C_{18} chromatography of the acid hydrolysate of adduct **3** demonstrating the presence of 8,9-dihydro-8-N^7-guanyl-9-hydroxy-AFB1. Chromatography conditions are as described in the text.

Scheme I. Synthetic Strategy for Formation of 8,9-Dihydro-8-{N^7-guanyl-[d(ATCGAT)]}-9-hydroxy-AFB1·d-(ATCGAT) (**3**) by Reaction with AFB1 8,9-Epoxide

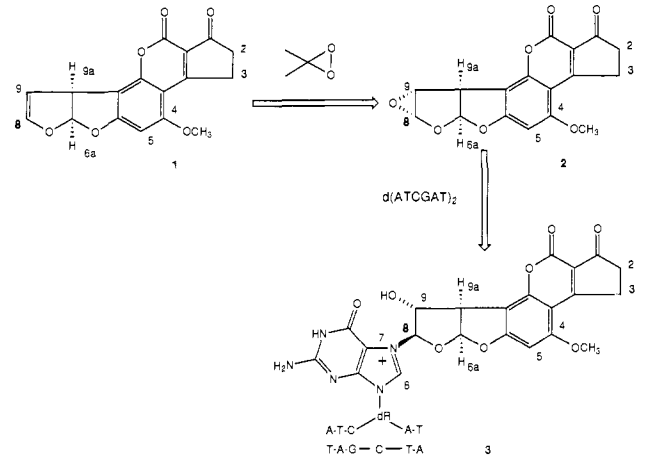

thermore, the products are consistent with regiospecific reaction of **2** at N^7 of guanine with inversion of configuration at C^8 of aflatoxin to yield the DNA adduct (for example, see **3**).

Other evidence for the pathway **1** → **2** → **3** illustrated in Scheme I has been derived from studies in which in situ activation of **1** has been carried out chemically. Procedures have included (1) oxidation by *m*-chloroperbenzoic acid (MCPBA),[3] (2) sensitized photooxidation,[4] and (3) solvolysis of 8-(acyloxy)-9-hydroxy derivatives of AFB1.[5] The in situ oxidation by MCPBA requires a two-phase system with the oxidant in methylene chloride solution to minimize oxidative degradation of the DNA. Analysis of DNA hydrolysates demonstrates that AFB1 adducts of DNA formed by MCPBA are identical with those obtained by enzymic activation,[6] but none have received detailed characterization prior to hydrolytic cleavage of the DNA. The yields of adducts produced by either chemical or enzymic in situ activation of **1** are too low to be practical for preparation of adducts with oligodeoxynucleotides on the scale required for characterization by NMR.

Many procedures for the preparation of epoxide **2** have been investigated but failed due to acidic constituents or nucleophiles in the reaction systems that caused cleavage of the epoxide.[6-9] We have recently developed a procedure for the synthesis of epoxide **2** permitting its isolation and characterization.[10] Although this epoxide is highly reactive, it is sufficiently stable that NMR spectra can be obtained at room temperature in nonnucleophilic solvents. The half-life in water is less than 10 s.[11] In spite of this facile hydrolysis, reaction occurs readily with DNA (in aqueous solution), indicating that DNA is able to compete effectively with the aqueous medium. In contrast to in situ enzymic or chemical activation of **1**, direct addition of the epoxide **2** to DNA or guanosine-containing duplex oligodeoxynucleotides in aqueous buffer results in high yields of the DNA adduct. We now report reaction of **2** with the DNA hexanucleotide duplex d(ATCGAT)$_2$ and characterization of the resulting adduct. The previously postulated structure **3** can now be viewed directly by NMR spectroscopy, which will allow the conformational consequences of adduct formation to be studied.

Materials and Methods

Materials. AFB1 was purchased from Sigma Chemical Co. Reagents for oligodeoxynucleotide synthesis were purchased from Pharmacia P. L. Biochemicals, Inc., and Fisher Scientific. d(ATCGAT) was synthesized by standard solid-phase phosphoramidite chemistry with an automated synthesizer. The amount of single-stranded d(ATCGAT) was determined by using a calculated extinction coefficient of 41 500 M^{-1} cm^{-1} at 260 nm.

Preparation of a d(ATCGAT)$_2$–AFB1 Adduct. All reactions with AFB1 were performed under subdued light to minimize potential formation of AFB1 photoproducts or photodecomposition of the resulting carcinogen–DNA adduct. A typical reaction was as follows. Dimethyldioxirane was prepared from potassium peroxysulfate as a distilled 0.05 M solution in acetone.[12] AFB1 (4.0 mg, 2.8 μmol), dissolved in 0.4 mL of methylene chloride, was converted to AFB1 8,9-epoxide by addition of 1.5 equiv of the dioxirane in acetone.[13] The reaction was complete within 15 min at room temperature, giving AFB1 8,9-epoxide

(3) Martin, C. N.; Garner, R. C. *Nature (London)* **1977**, *267*, 863–865.
(4) Büchi, G.; Fowler, K. W.; Nadzan, A. M. *J. Am. Chem. Soc.* **1982**, *104*, 544–547.
(5) Coles, B. F.; Welch, A. M.; Hertzog, P. J.; Lindsay Smith, J. R.; Garner, R. C. *Carcinogenesis* **1980**, *1*, 79–89.
(6) Garner, R. C.; Martin, C. N.; Lindsay Smith, J. R.; Coles, B. F.; Tolson, M. R. *Chem.-Biol. Interact.* **1979**, *26*, 57–73.
(7) Gorst-Allman, C. P.; Steyn, P. S.; Wessels, P. L. *J. Chem. Soc., Perkin Trans. 1* **1977**, 1360–1364.
(8) Coles, B. F.; Lindsay Smith, J. R.; Garner, R. C. *J. Chem. Soc., Perkin Trans. 1* **1979**, 2664–2671.
(9) Miller, J. A. *Cancer Res.* **1970**, *30*, 559–576.
(10) Baertschi, S. W.; Raney, K. D.; Stone, M. P.; Harris, T. M. *J. Am. Chem. Soc.* **1988**, *110*, 7929–7931.
(11) Baertschi, S. W.; Raney, K. D.; Shimada, T.; Harris, T. M.; Guengerich, F. P. *Chem. Res. Toxicol.* **1989**, *2*, 114–122.
(12) Murray, R. W.; Jeyaraman, R. *J. Org. Chem.* **1985**, *50*, 2847–2853. Adam, W.; Chan, Y.-T.; Cremer, D.; Gauss, J.; Scheutzow, D.; Schindler, M. *J. Org. Chem.* **1987**, *52*, 2800–2803. Baumstark, A. L.; Vasquez, P. C. *J. Org. Chem.* **1988**, *53*, 3437–3439.
(13) *Caution*: Crystalline aflatoxin B_1 is extremely hazardous due to its carcinogenicity and electrostatic nature and should be handled by appropriate containment procedures and respiratory mask to prevent inhalation. The toxicological properties of the epoxide **2** are presently being investigated. It should be assumed that **2** is highly toxic and carcinogenic. Manipulations should be carried out in a well-ventilated hood with use of disposable latex gloves. Aflatoxins can be destroyed by treatment with commercial NaOCl solutions.

Chart I

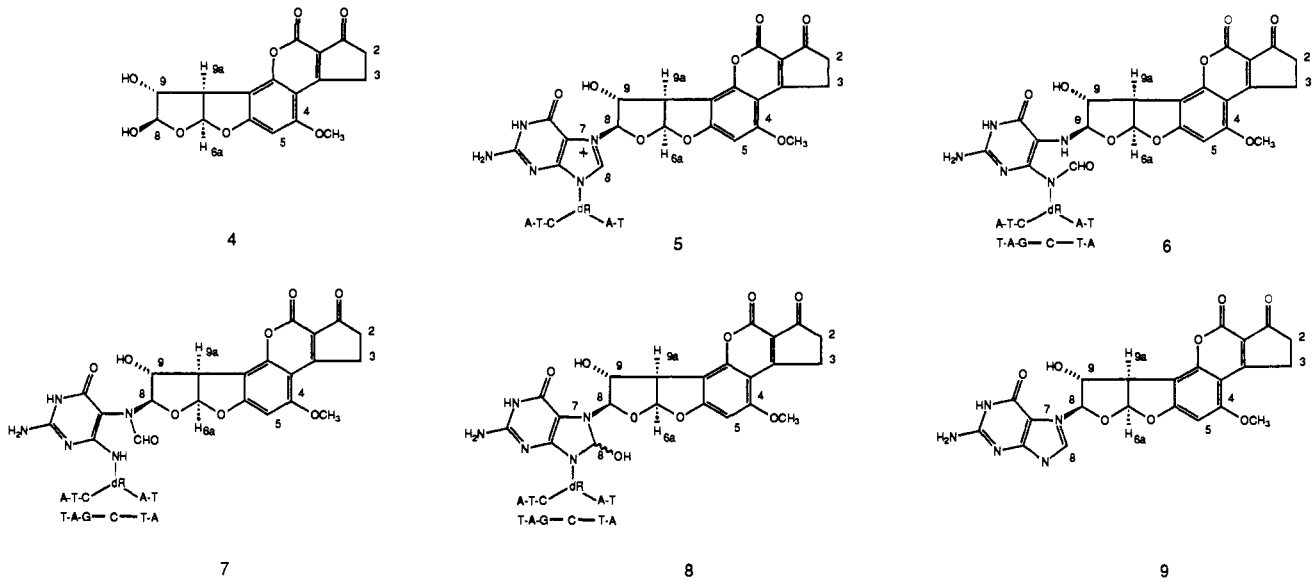

and acetone as the only products. The solution was evaporated to dryness under a stream of N_2 to remove excess dioxirane. The residue of AFB1 8,9-epoxide was redissolved in 0.5 mL of dichloromethane. AFB1 8,9-epoxide (12.8 μmol) in dichloromethane was added to d(ATCGAT) (75 A_{260} units, 1.8 μmol) dissolved in 0.5 mL of a 0.01 M sodium phosphate buffer, pH 7.0, containing 0.1 M NaCl and 5×10^{-5} M disodium ethylenediaminetetraacetic acid (EDTA) at 5 °C with vigorous shaking for 5 min. The aqueous and organic layers were separated; AFB1 8,9-dihydrodiol was removed by extraction into methylene chloride. Alternatively, gel filtration of the aqueous phase through Bio-Gel P-2 equilibrated at 5 °C with 0.01 M sodium phosphate buffer, pH 6.8, yielded $d(ATCGAT)_2$ and $d(ATCGAT)_2$–AFB1 in the void volume fraction that was collected and lyophilized.

Purification of the Adduct. The limiting stoichiometry of adduct formation was determined to be 1:1 AFB1 to $d(ATCGAT)_2$ by repeated treatment of $d(ATCGAT)_2$ with **2**, which showed that no further reaction with epoxide occurred after 50% of the strands had been modified. In initial experiments, the crude reaction mixture obtained after two to three additions of epoxide **2** was purified by gel filtration and examined directly. This approach proved unsatisfactory because small quantities of impurities were typically observed (Figure 1A). These impurities, primarily depurination products, arise due to the instability of purine N^7-alkyl derivatives. In other experiments, the modified and unmodified strands were initially purified by C_{18} HPLC (C_{18}, Alltech Associates, 5–25% CH_3CN gradient; 3.0 mL/min; 25 min), followed by titration of freshly purified d(ATCGAT)–AFB1 into $d(ATCGAT)_2$ at 5 °C. The progress of the titration was monitored by integration of ^1H NMR signals arising from $d(ATCGAT)_2$ and $d(ATCGAT)_2$–AFB1, which were in slow exchange on the NMR time scale. No difference in the ^1H NMR spectrum of adduct **3** as compared to the corresponding signals in NMR samples prepared directly from the crude reaction mixture was observed.

Optical Spectroscopy. UV–vis spectroscopic measurements were made on a Varian Cary 2390 spectrophotometer interfaced with a Neslab ETP-3 temperature programmer unit for performing melting experiments. CD measurements were made with a Jasco 500A scanning spectropolarimeter. Optical measurements on the double-stranded species [both $d(ATCGAT)_2$ and $d(ATCGAT)_2$–AFB1 adducts] were made by dilution of concentrated solutions into 1 M NaCl buffer to favor maintenance of duplex conformation at the low concentrations used for optical spectroscopy.

Nuclear Magnetic Resonance. ^1H NMR frequencies of 300.13 or 400.13 MHz were utilized. ^{31}P NMR was performed at 162 MHz. Samples were dissolved in NMR buffer consisting of 0.1 M NaCl, 5×10^{-5} M Na_2EDTA, and 0.01 M sodium phosphate, pH 7.0. Samples were lyophilized three times from D_2O and then dissolved in 400 μL of 99.96% D_2O. For observation of the exchangeable ^1H resonances, samples were dissolved in H_2O containing 10% D_2O and spectra were run in the 1331 water suppression pulse sequence.[14] Chemical shifts were referenced internally to DSS; sample temperature was controlled within 0.5 °C.

(14) Hore, P. J. *J. Magn. Reson.* **1983**, *54*, 539–542. Hore, P. J. *J. Magn. Reson.* **1983**, *55*, 283–300.

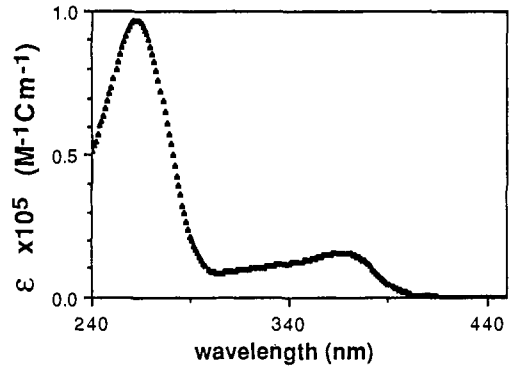

Figure 2. UV–vis spectrum of adduct **3** at 5 °C in 1 M NaCl buffer.

Results

Formation of a Covalent Adduct. Addition of **2** to $d(ATCGAT)_2$ by the procedure described above proved to be a facile and readily reproducible method for generating an intact oligodeoxynucleotide adduct. Competing hydrolysis of **2** by the large molar excess of water to form AFB1 8,9-dihydrodiol (**4**) destroys unreacted epoxide; diol **4** represents the principal byproduct in the reaction of the epoxide with DNA and was removed from the reaction mixture by extraction or by gel filtration. The presence of covalent adducts was monitored by observation of nonextractible absorbance at 360 nm. Reaction of **2** with the oligodeoxynucleotide proceeded efficiently despite the presence of a large molar excess of water; two to three additions of epoxide yielded the limiting stoichiometry of 1:1 AFB1 to $d(ATCGAT)_2$.

UV–vis, CD, and HPLC Analyses. The principal product was identified as the double-stranded monoadduct 8,9-dihydro-8-{N^7-guanyl[d(ATCGAT)]}-9-hydroxy-AFB1·d(ATCGAT) (**3**), by UV spectroscopy, circular dichroism measurements, reversed-phase chromatography, and ion-exchange chromatography. The UV spectrum of **3** is shown in Figure 2. UV absorption maxima were observed at 262 and at 367 nm. The ratio of A_{262} to A_{367} was 6.1; the A_{260} to A_{280} ratio was 1.8. The extinction coefficient at 262 nm for the double-stranded adduct was measured to be 9.6×10^4 M^{-1} cm^{-1}; the extinction coefficient at 367 nm was 1.5×10^4 M^{-1} cm^{-1}. No absorbance was observed at wavelengths greater than 420 nm, and the color of the sample was pale yellow. No fluorescence was observed for adduct **3**.

Figure 3 shows the CD spectrum of $d(ATCGAT)_2$ compared with adduct **3**. The unreacted oligodeoxynucleotide exhibits a CD spectrum characteristic of a B-DNA helix. Adduct **3** exhibits negative ellipticity centered at 362 nm, which is assigned to the AFB1 coumarin chromophore. The presence of the bound AFB1

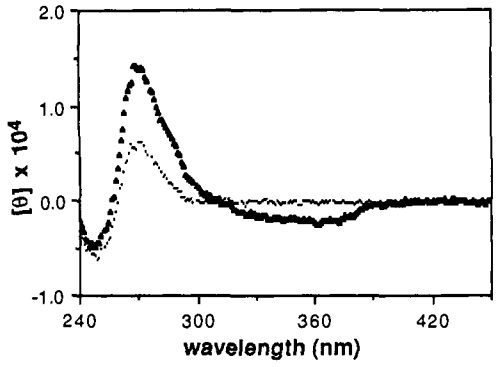

Figure 3. CD spectrum of adduct 3 (solid triangles) as compared to d(ATCGAT)$_2$ (dotted line). Both spectra were obtained at 5 °C in 1 M NaCl buffer.

moiety induces changes in the CD spectrum between 230 and 300 nm; the positive CD band at 269 nm increases in intensity, whereas the magnitude of the negative ellipticity at 250 nm is not substantially altered. The crossover point between positive and negative ellipticity is unchanged.

Reversed-phase HPLC analysis of 3 yielded two fractions of approximately equal area (Figure 1B). The peak eluting at 12% acetonitrile was identified as unreacted d(ATCGAT) since it coeluted with and had the same UV spectrum as an authentic sample of d(ATCGAT). The second peak, identified as the single-stranded adduct 8,9-dihydro-8-{N^7-guanyl[d-(ATCGAT)]}-9-hydroxy-AFB1 (**5**), eluted at 16% acetonitrile with maximum absorbances at 262 and 365 nm. Figure 4 shows the UV spectra for the two peaks obtained in the HPLC chromatogram. The ratio of A_{262} to A_{365} for the second peak was measured to be 3.7.

Anion-exchange HPLC of 3 is shown in Figure 1C; again two fractions were obtained. Peak 1, which eluted at 13 min (0.95 M ammonium acetate), was identified by UV spectroscopy as the single-strand adduct **5**. Peak 2, which eluted at 17 min (1.0 M ammonium acetate), was identified by the UV spectrum as unreacted single-strand d(ATCGAT). It is noteworthy that the single-strand adduct **5** eluted from the SAX column before unreacted d(ATCGAT), whereas on the C_{18} column it eluted subsequent to d(ATCGAT). This observation supports the assignment of 3 as the cationic N^7-guanyl-AFB1 adduct, rather than the neutral formamidopyrimidine (FAPY) products (**6**, **7**) or the C^8-hydroxylated products (**8**) that could be formed by attack of hydroxide at the C^8-position of the modified guanine nucleotide in species 3. This assignment is further supported by NMR and UV analysis of the acid hydrolysate of 3.

Acid Hydrolysis of Adduct 3. An aliquot of adduct 3 was hydrolyzed by adjustment to pH 1.5 with HCl, followed by heating at 70 °C for 20 min. The pH of the solution was readjusted to neutrality, and the solution was filtered through a 0.22-μm filter. The acid hydrolysate was applied to a reversed-phase HPLC column equilibrated with 0.01 M sodium phosphate, pH 6.5. The hydrolyzed adduct was eluted with a gradient of 10–80% acetonitrile in 40 min (Figure 1D). The acid hydrolysate of 3 yielded a product eluting at 14 min corresponding to the previously identified 8,9-dihydro-8-(N^7-guanyl)-9-hydroxy-AFB1 (**9**).[2a,b] This peak coeluted with a known standard sample of **9**, and the assignment was confirmed by UV and NMR spectroscopies. No other products of acid hydrolysis of 3 were detected containing the 360-nm coumarin chromophore, indicating that adduct 3 is a pure species and not a mixture of cationic and FAPY species.

Mild Base Hydrolysis of the Cationic Adduct 3. Adduct 3 was transformed by basic hydrolysis to yield products assigned as FAPY derivatives **6** and **7**. When adduct 3 was adjusted to pH 8.0 with NaOH, no reaction was observed at room temperature, but gentle heating (30 °C for 19.5 h) of the sample, followed by readjustment of the pH to neutrality and reversed-phase HPLC, showed that the peak for strand **5** was reduced in area in the C_{18} chromatogram while two additional peaks eluting prior to **5** appeared. These new peaks upon acid hydrolysis gave the FAPY derivative as identified by its reported UV spectrum.[2b] Likewise, anion-exchange HPLC showed a reduction in area for strand **5** and appearance of a new peak, considered to be the FAPY derivative. Its retention time was similar to that of unmodified d(ATCGAT).

Thermodynamic Stability of the AFB1–d(ATCGAT)$_2$ Adduct (3). Optical melting experiments were performed on 3 μM (duplex) samples of the unmodified oligodeoxynucleotide d-(ATCGAT)$_2$ and adduct 3 in 1 M NaCl buffer (Figure 5). Under these conditions, both d(ATCGAT)$_2$ and adduct 3 show broad melting transitions, for which the upper and lower base lines of the melting curve are not reached. T_m for d(ATCGAT)$_2$ is ~15 °C. Formation of 3 results in a small but significant increase in the T_m to ~19 °C. Thus, 3 is thermodynamically more stable than the unmodified duplex. Quantitative analysis of the melting data was not attempted due to the broad nature of the melting transitions. It is likely that a small amount of depurination of adduct 3 occurred during the course of the melting experiment, which required approximately 80 min, as evidenced by the observation that the absorbance upon returning to low temperature subsequent to the melt was slightly altered.

^{1}H NMR of Adduct 3. NMR spectroscopy provides further support that adduct 3 is double-stranded. Figure 6 shows the results of a titration of d(ATCGAT)$_2$ with d(ATCGAT)–AFB1 (**5**). Addition of the modified strand **5** results in the appearance of a new set of resonances in the ^{1}H NMR spectrum and disappearance of those characteristic of unmodified duplex. The second set of resonances is observed both for the nonexchangeable protons and for the exchangeable hydrogen-bonded protons. The new resonances arise from hybrid duplex 3; observation of two subspectra indicates that strand exchange between duplex 3 and unmodified d(ATCGAT)$_2$ is slow on the NMR time scale.

Figure 7 shows the aromatic region of the ^{1}H NMR spectra of unreacted d(ATCGAT)$_2$ and adduct duplex 3. Assignments for key protons in adduct 3 are shown in Figure 7; the assignments

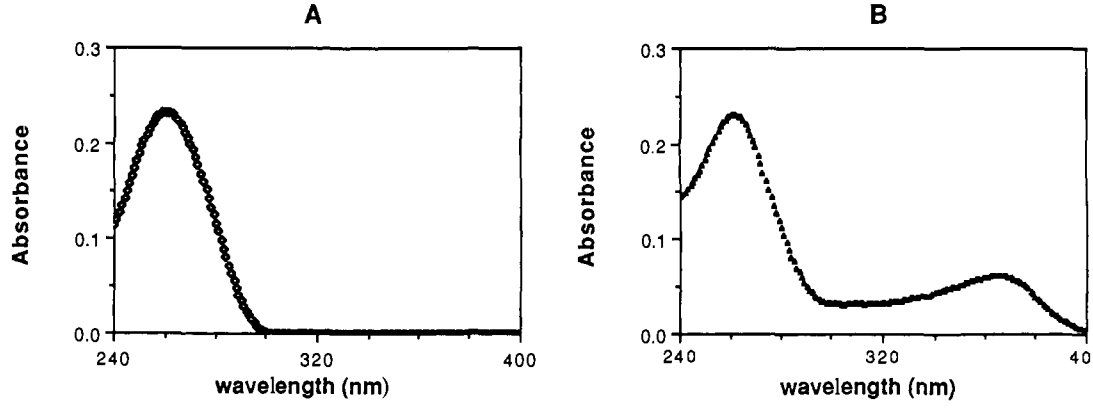

Figure 4. UV–vis spectra of the two individual strands from adduct 3 as separated by reversed-phase HPLC chromatography shown in Figure 1B. The spectra were run at 5 °C in 1 M NaCl buffer.

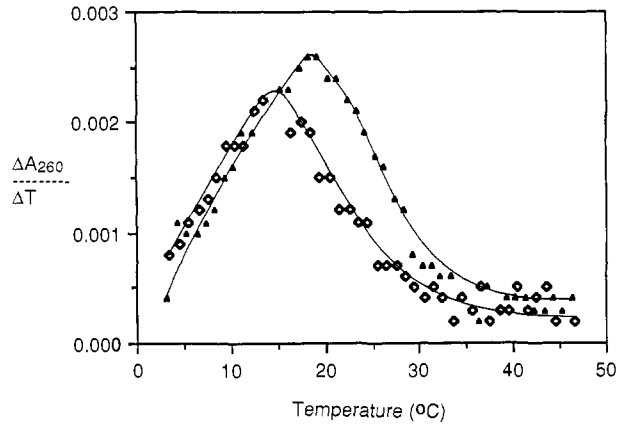

Figure 5. Melting profiles of $d(ATCGAT)_2$ (diamonds) and adduct **3** (▲) plotted as the first derivative of absorbance change vs temperature.

were made by comparison with the spectrum of $d(ATCGAT)_2$ and from inspection of scalar coupling data, NOE difference spectra, and nonselective T_1 relaxation experiments. These assignments are briefly described in the following paragraphs.

Covalent attachment of AFB1 to the oligodeoxynucleotide results in a doubling of the oligodeoxynucleotide resonances due to loss of the pseudodyad symmetry axis of the self-complementary sequence. Two cytosine H6 doublets are observed at 7.60 and 7.75 ppm. The thymine H6 signals are observed in two groups of two signals, at 7.20/7.25 and 7.40/7.45 ppm; the 5-CH_3 signals are incompletely resolved as pairs at 1.32 and 1.18 ppm (data not shown). The adenine H2 protons, identified from T_1 measurements, are broken into two sets of signals observed at 7.8 and 8 ppm. The adenine H8 protons are observed in a cluster from 8.1 to 8.3 ppm. One guanine H8 proton is observed at 7.88 ppm whereas the second GH8 proton is not observed with the sample in D_2O. Loss of the guanine H8 proton at the site of reaction is consistent with formation of an N^7 adduct, which would render the H8 proton more acidic and subject to facile exchange with D_2O. The observed spectrum is consistent with formation of an adduct at N^7 of guanine.

An additional signal, which is tentatively assigned as the fugitive GH8, was observed at 9.75 ppm in the H_2O spectrum (Figure 6B). This signal, which is only observed in H_2O solution, is not observed in unreacted $d(ATCGAT)_2$ and disappears upon basic hydrolysis of the adduct to form the FAPY derivative. It is shifted significantly downfield with respect to the five identified purine H8 protons. The observation of this signal in H_2O and its downfield shift are consistent with the hypothesis that in the cationic adduct the H8 proton of the modified guanine has increased acidity and exchanges with solvent but that this exchange is sufficiently slow so as to be observed in H_2O solution. The exchange rate of this proton is judged to be rapid from an experiment in which the water signal was saturated; under these conditions neither the imino proton signals nor the 9.75 ppm signal was observed due to saturation transfer from water.

Additional evidence in support of a double-stranded conformation for adduct **3** is derived from analysis of ^1H NMR spectra in H_2O, in which hydrogen-bonded resonances in slow exchange with solvent are observed (Figures 6B and 8). Signals from six imino hydrogen bonded protons are observed at −10 °C (Figure 8) in the region between 12 and 14 ppm; the generation of six signals is a result of the loss of symmetry upon adduct formation. The presence of these six signals argues that binding of AFB1 has not disrupted the base pairing of the DNA duplex and strongly supports the interpretation that **3** is a duplex species.

The resonances from the aflatoxin moiety in the double-stranded cationic adduct **3** were identified from scalar coupling patterns

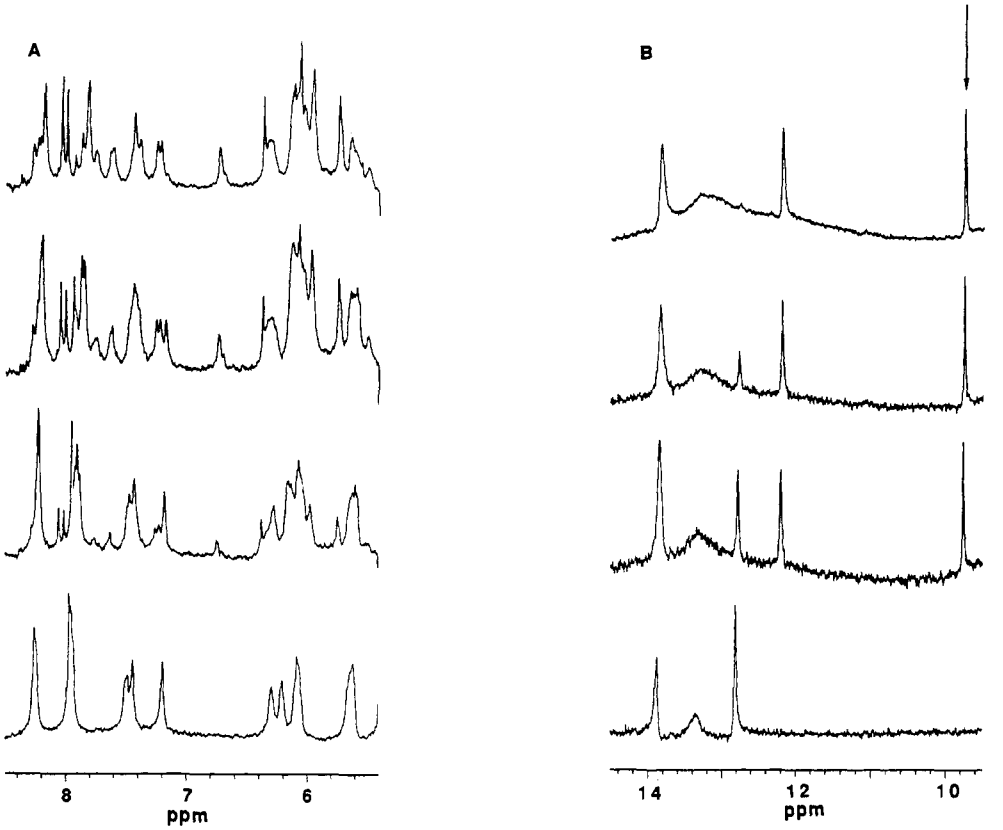

Figure 6. Titration of adduct **5** into $d(ATCGAT)_2$ as monitored by ^1H NMR spectroscopy at 5 °C. The titration proceeds from bottom to top in each panel, where the bottom trace represents $d(ATCGAT)_2$. Key: (A) nonexchangeable base and sugar anomeric protons in D_2O; (B) exchangeable hydrogen-bonded protons in 90% H_2O–10% D_2O. As modified strand **5** is added to the solution, resonances from adduct **3** appear, in slow exchange with those arising from $d(ATCGAT)_2$. Simultaneously, resonances arising from $d(ATCGAT)_2$ decrease in intensity. Formation of a 2:1 AFB1 to $d(ATCGAT)_2$ complex is not observed. An additional signal is observed at 9.75 ppm in the 90% H_2O spectrum of adduct **3** (see arrow) and is tentatively identified as GH8 of the modified guanine. This signal disappears from the spectrum upon mild basic hydrolysis of adduct **3**.

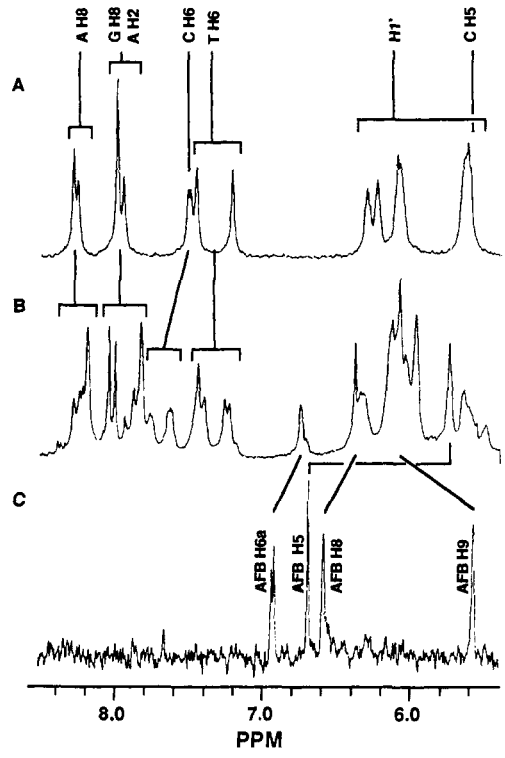

Figure 7. ^{1}H NMR spectra at 5 °C of (A) d(ATCGAT)$_2$, (B) adduct **3**, and (C) AFB1. Formation of adduct **3** results in a doubling of the oligodeoxynucleotide resonances. See Scheme I for the numbering system used for the AFB1 protons.

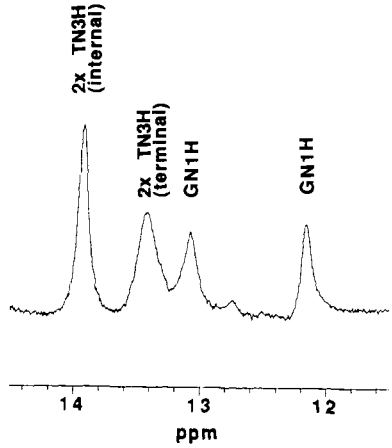

Figure 8. ^{1}H NMR spectrum at −10 °C of adduct **3** showing the presence of six hydrogen-bonded protons. Formation of adduct **3** does not resolve the imino proton resonances arising from the terminal or internal A–T base pairs but does resolve the two G–C imino proton resonances.

and NOE difference data. The AFB1 H6a proton observed at 6.74 ppm exhibited coupling to the AFB1 H9a proton at 3.93 ppm. Likewise, coupling was observed between AFB1 H8 (6.37 ppm) and AFB1 H9 (6.06 ppm). Observation of the furan ring coupling pattern confirmed that the AFB1 moiety in the covalent adduct was intact; i.e., opening of the furan ring to an aldehyde had not occurred. The AFB1 H5 aromatic proton at 5.73 ppm was identified from an NOE difference spectrum, which showed an NOE to the 4-OCH_3 protons, located at 3.63 ppm. The methylenic protons at C^2 and C^3 of AFB1 were not identified due to overlap with deoxyribose H2′ and H2″ protons.

Several small additional signals are observed in Figures 6–8 that reflect the presence of impurities. On the basis of HPLC analyses of the NMR sample, these impurities are judged to have arisen from depurination of modified strand **5**, resulting in formation of d(ATC-deoxyribose-AT) and 8,9-dihydro-8-N^7-guanyl-9-hydroxy-AFB1 (**9**). Maintenance of the sample at <5 °C is essential to minimize depurination of the adducted strand; NMR samples were stored at −20 °C between experiments. Additional signals can also arise from inexact adjustment of the ratio of modified strand **5** to unmodified strand.

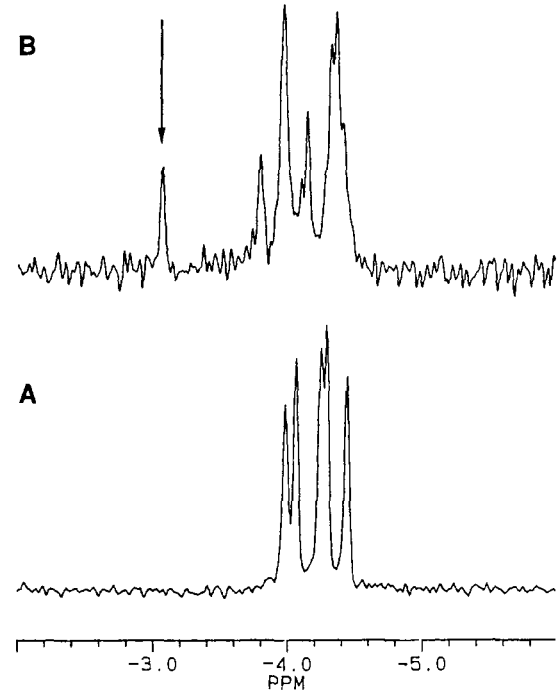

Figure 9. ^{31}P NMR spectra at 5 °C of (A) d(ATCGAT)$_2$ and (B) adduct **3**. For the unmodified oligodeoxynucleotide, five ^{31}P signals are resolved; for nonsymmetrical adduct **3**, ten signals are present. Formation of adduct **3** results in a substantial downfield shift for at least one ^{31}P resonance as denoted by the arrow.

^{31}P NMR Analysis of Adduct 3. Figure 9 shows the ^{31}P spectrum of double-stranded adduct **3** as compared to d(ATCGAT)$_2$. Formation of adduct **3** results in substantial deshielding of one phosphorus nucleus whose resonance is observed at −3 ppm (TMP reference; see arrow in Figure 9). A second ^{31}P resonance is slightly deshielded and appears at −3.8 ppm. Interpretation of the ^{31}P spectrum is beyond the scope of the present study.

Discussion

Several considerations indicated that d(ATCGAT)$_2$ would be a useful sequence for an initial study of reactivity of the epoxide. First, the sequence is self-complementary, obviating the need to synthesize and combine two differing but complementary oligomers in stoichiometric amounts. Second, the two guanines in the duplex, i.e., one in each chain, are identical, avoiding potential problems with regioselectivity if two distinguishable guanines are present. Finally, the sequence 5′-CpG-3′ has been reported to be a preferred site for binding of aflatoxin epoxide.[15]

Chemical and Thermodynamic Stability of Double-Stranded Adduct 3. The positive charge localized on the imidazole ring of the modified guanine in **3** potentially leads to three types of chemical instability:[1,2] (1) cleavage of the aflatoxin moiety from N^7 to give diol **4** and unmodified oligomer, (2) hydroxide attack at C^8 with ensuing ring opening to give formamidopyrimidine adducts **6** and **7**, and (3) cleavage of the deoxyribose moiety from N^9 to give **9** and the apurinic oligomer. When the sample was maintained at pH <8, formation of diol **4** and FAPY **6** and **7** was not observed. In contrast, cleavage at N^9 was a major process and the sample had to be maintained at low temperature to prevent depurination. Above pH 8 FAPY formation occurred and become rapid when the sample was warmed.

Addition of epoxide **2** to d(ATCGAT)$_2$ could have created a complex equilibrium mixture of single-strand and duplex forms of modified and unmodified strands (Scheme II). Dissociation of adduct **3** would yield d(ATCGAT) and d(ATCGAT)–AFB1 (**5**). Each of these strands has the potential for self-association.

Scheme II

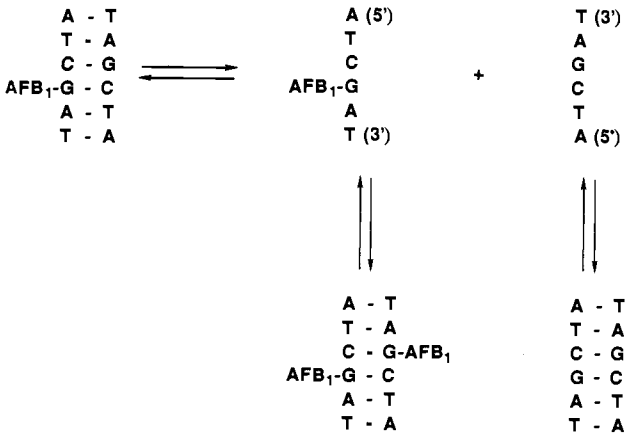

Our results suggest that equilibrium between double-stranded adduct **3** and its component strands favors maintenance of a double-stranded duplex in which only one strand is modified. This conclusion is based upon observations that the modified duplex has increased thermodynamic stability and that the limiting stoichiometry of the reaction of **2** with $d(ATCGAT)_2$ is 1:1 AFB1 to $d(ATCGAT)_2$. If modification had destabilized $d(ATCGAT)_2$, disproportionation into single-stranded adduct **5** and unreacted $d(ATCGAT)_2$ would have occurred and it should then have been possible to force greater than 50% of the strands to react with **2**. Titration of **5** into d(ATCGAT) resulted only in the formation of the more stable double-stranded adduct **3**, as monitored by NMR spectroscopy (Figure 6).

Association of AFB1 8,9-Epoxide (2) with Duplex DNA. The association of epoxide **2** with DNA cannot be directly examined due to the reactivity of the epoxide. Indirect evidence derived from binding studies[17-22] using AFB1 as a surrogate for the reactive epoxide suggests that **2** may intercalate into DNA. AFB1 binds to poly(dGdC)·poly(dG:dC), poly(dAdT)·poly(dAdT), and calf thymus DNA. These complexes have association constants of $\sim 10^3$ M^{-1}. Disruption of the B-DNA duplex structure causes concurrent dissociation of AFB1 from DNA.[21,22] Association of AFB1 with $d(ATCGAT)_2$ results in increased shielding for each of the AFB1 protons; this increase is as large as 0.82 ppm for the H5 proton of AFB1. Similar chemical shift changes observed for association of AFB1 with the isomeric sequence $d(ATGCAT)_2$ have been interpreted in terms of an intercalated complex; that conclusion received support from longitudinal relaxation measurements, competitive binding experiments, and electrophoretic studies of supercoiled and relaxed closed-circular pBR322 DNA.[22]

Reaction of AFB1 8,9-Epoxide (2) with $d(ATCGAT)_2$. Prior to development of the direct route to adduct **3** outlined in Scheme I, we attempted to prepare **3** by in situ generation of epoxide **2** by addition of MCPBA to a two-phase CH_2Cl_2/H_2O solution containing AFB1 and $d(ATCGAT)_2$ buffered at pH 7.[3,6] Although adduct **3** was obtained, indirect generation of **2** proved inefficient and difficult to control, often leading to decomposition of the oligodeoxynucleotide. The decomposition processes were not investigated but were presumed to result from oxidation of the oligodeoxynucleotide by the peroxy acid.[23]

Table I. Comparison of Chemical Shift Changes of Various AFB1 Resonances upon Formation of **3** and the Corresponding Associative Complex between AFB1 and $d(ATCGAT)_2$ (Temperature Maintained at 5 °C)

proton	σ_{free}[a]	$\delta_{covalent}$[b]	$\Delta\delta_{cov}$	$\delta_{noncovalent}$[c]	$\Delta\delta_{noncovalent}$
H6a	6.93	6.75	−0.18	6.72	−0.21
H5	6.69	5.75	−0.94	5.87	−0.82
H9a	4.8[d]	3.95	−0.85	4.47	−0.33
4-OCH_3	3.98	3.65	−0.33	3.62	−0.36
H8[e]	6.59	6.38	−0.21[e]	6.49	−0.10
H9[e]	5.57	6.08	+0.51[e]	5.37	−0.20

[a] Saturated solution of AFB1 dissolved in D_2O buffered as described in the text. [b] The concentration of **3** was 2.0 mM. [c] Chemical shifts measured from an equilibrium mixture containing 2.0 mM $d(ATCGAT)_2$ in the presence of a saturated solution of AFB1. The equilibrium is rapid on the NMR time scale; chemical shifts represent weighted averages of free and bound AFB1. [d] Estimated chemical shift. This signal is located beneath the solvent resonance in D_2O. In DMSO-d_6 the H9a signal is observed at 4.75 ppm. [e] C^8 and C^9 of AFB1 change hybridization upon formation of **3**.

Double-stranded DNA is required to obtain efficient formation of the aflatoxin adduct.[15a] The low duplex stability of $d(ATCGAT)_2$ ($T_m < 30$ °C at NMR concentrations) dictated that reaction with epoxide should be performed at low temperature. Duplex stability could be increased by raising the ionic strength of the media, but association of AFB1 with DNA decreases at higher ionic strength.[21] Thus, the effect of ionic strength may be complex. A salt concentration of 0.1 M was chosen for the present study.

The stereochemistry of epoxide opening by DNA is exclusively trans,[2] whereas on the basis of solvolysis studies carried out by Coles et al.[8] one would expect to obtain a mixture of cis and trans adducts with DNA. For stereospecific formation of the observed adduct, **2** must be constrained such that the guanine N^7 nucleophile is delivered from the more hindered endo side, i.e., with the trajectory of attack lying in a plane parallel to the coumarin nucleus. The efficiency of reaction between labile epoxide **2** and DNA is remarkable[10] and suggests facile formation of a favorable transition state complex.[15a,c,24]

Loechler and co-workers have proposed that this high efficiency of reaction reflects association of **2** with the DNA, which raises its local concentration.[15c] Furthermore, they propose that AFB1 epoxide is held in an orientation promoting reaction. This hypothesis could explain not only the reaction efficiency but also the stereospecificity of the epoxide opening and the observed regioselectivity in which guanines in some sequences are significantly more reactive than in others.[24] Loechler et al. have conducted molecular modeling studies to examine potential transition states, concentrating primarily upon those involving major-groove binding, to explain the observed sequence specificity of adduct formation.[25]

The present experimental studies cannot define the structure of the transition state. However, on the basis of our experimental evidence, we favor a model in which the transition state complex between **2** and $d(ATCGAT)_2$ involves intercalation. The similarity in chemical shift changes (Table I) for AFB1 noncovalently bound and covalently linked to $d(ATCGAT)_2$ suggests that the associative complex and adduct **3** have similar geometry. As discussed in the preceding section, binding experiments in which AFB1 was used as a surrogate for **2** are consistent with intercalative association.[22] The limiting stoichiometry of 1:1 AFB1 to $d(ATCGAT)_2$ in the formation of **3** reveals that the bonded af-

(15) (a) Misra, R. P.; Muench, K. F.; Humayun, M. Z. *Biochemistry* **1983**, *22*, 3351–3359. (b) Marien, K.; Moyer, R.; Loveland, P.; Van Holde, K.; Bailey, G. *J. Biol. Chem.* **1987**, *262*, 7455–7462. (c) Benasutti, M.; Ejadi, S.; Whitlow, M. D.; Loechler, E. L. *Biochemistry* **1988**, *27*, 472–481.

(16) For a review, see: Rodricks, J. V., Hesseltine, C. W., Mehlman, M. A., Eds. *Proceedings of the Conference on Mycotoxins in Human and Animal Health*; Pathotex Publishers: Park Forest South, Il, 1977.

(17) Clifford, J. I.; Rees, K. R. *Nature (London)* **1966**, *209*, 312–313. Clifford, J. I.; Rees, K. R. *Biochem. J.* **1967** *103*, 467–471.

(18) Sporn, M. B.; Dingman, C. W.; Phelps, H. L.; Wogan, G. N. *Science* **1966**, *151*, 1539–1541.

(19) Neely, W. C.; Lansden, J. A.; McDuffie, J. R. *Biochemistry* **1970**, *9*, 1862–1866.

(20) Clifford, J. I.; Rees, K. R.; Stevens, M. E. M. *Biochem. J.* **1967**, *103*, 258–261.

(21) Stone, M. P.; Gopalakrishnan, S.; Harris, T. M.; Graves, D. E. *J. Biomol. Struct. Dyn.* **1988**, *5*, 1025–1042.

(22) Gopalakrishnan, S.; Byrd, S.; Stone, M. P.; Harris, T. M. *Biochemistry* **1989**, *28*, 726–734.

(23) Jacobsen, J. S.; Humayun, M. Z. *Carcinogenesis* **1986**, *7*, 491–493.

(24) For an excellent discussion of the factors influencing adduct formation, see: Warpehoski, M. A.; Hurley, L. H. *Chem. Res. Toxicol.* **1988**, *1*, 315–333.

(25) Loechler, E. L.; Teeter, M. M.; Whitlow, M. D. *J. Biomol. Struct. Dyn.* **1988**, *5*, 1237–1257.

latoxin moiety is oriented such that the guanine in the complementary strand is sterically inaccessible to attack by epoxide **2**; i.e., the presence of AFB1 covalently linked to one guanine in d(ATCGAT)$_2$ precludes a second molecule of AFB1 epoxide from achieving the transition state with the other guanine. Intercalation of the aflatoxin moiety in adduct **3** above the 5′ face of the modified guanine would be consistent with this observation and represents an attractive hypothesis with which to explain the observed stoichiometry of adduct formation. Thus, existing experimental data regarding the geometry of the associative AFB1–d(ATCGAT)$_2$ complex and of covalent adduct **3** are similar and more consistent with intercalation than with groove binding. It therefore seems plausible that the transition state for reaction of epoxide **2** with DNA, although not directly observable, also involves intercalation.

The accessibility of chemically discrete AFB1–oligodeoxynucleotide adducts will now permit detailed conformational analysis by NMR spectroscopy. Further study of adduct **3** will establish its three-dimensional structure with certainty.

Acknowledgment. This research has been funded by the National Institutes of Health, Grants ES-03755 and ES-00267. We thank Professor Fu-Ming Chen (Tennessee State University) for providing assistance in obtaining CD spectra and Dr. Steven W. Baertschi for advice on preparation of dimethyldioxirane and epoxide **2**.

Mössbauer Analysis of the Binuclear Iron Site in Purple Acid Phosphatase from Pig Allantoic Fluid

J. T. Sage,[1a,b] Y.-M. Xia,[1a] P. G. Debrunner,*[,1a] D. T. Keough,[1c] J. de Jersey,[1c] and Burt Zerner*[,1c]

Contribution from the Department of Physics, University of Illinois, Urbana, Illinois 61801, and the Department of Biochemistry, University of Queensland, St. Lucia, Queensland, Australia 4067. *Received March 29, 1988*

Abstract: We present a quantitative analysis of the Mössbauer spectra of the spin-coupled two-iron center in porcine purple acid phosphatase. The active enzyme contains a high-spin Fe(III)–Fe(II) pair with a ground state of effective spin $S = {}^1/_2$ and **g** tensor $g = (1.56, 1.72, 1.93)$, while the oxidized, inactive enzyme contains a high-spin Fe(III)–Fe(III) pair with a diamagnetic ground state. The Mössbauer spectra of reduced enzyme recorded at 4.2 K show complex magnetic hyperfine splittings, which have been parametrized in terms of the spin Hamiltonian $H = \beta \mathbf{S} g \mathbf{B} + \sum_i \mathbf{S} A_i \mathbf{I}_i + \sum_i \mathbf{I}_i P_i \mathbf{I}_i - \sum_i \beta_N g_N \mathbf{I}_i \mathbf{B}$, $S = {}^1/_2$, where i = A and B labels the ferric and ferrous site, respectively. The fitting parameters **g** and A_i can, in turn, be related to the intrinsic tensors g_i and a_i of the ferric and ferrous ions, respectively, assuming the coupling $H = -2J\mathbf{S}_A\mathbf{S}_B + \sum_i \mathbf{S}_i D_i \mathbf{S}_i$ between the intrinsic spins $S_A = {}^5/_2$ and $S_B = 2$. With the estimate $-2J = 20$ cm^{-1} (Lauffer et al. *J. Biol. Chem.* **1983**, *258*, 14212–14218) and reasonable zero-field splittings D_i, the model explains the low g values and the unusual anisotropy of the ferric hyperfine tensor A_A in the coupled representation. Explicit expressions for the tensors **g** and A_i are given to first order in D_i/J. this intermediate coupling model, $|D_i/J| \lesssim 1$, is likely to apply to semimethemerythrins, methane monooxygenase, and other high-spin Fe(III)–Fe(II) couples with **g** values differing widely from $g = 2$ and to hold the key to a quantitative interpretation of susceptibility, ENDOR, and other magnetic properties. Preliminary data for metal-substituted and differentially enriched phosphatase are also presented. The parameters of the iron in the Fe–Zn enzyme are found to be close to the intrinsic parameters deduced from the analysis of the native Fe(III)–Fe(II) enzyme, a result that not only corroborates our model but also indicates little change in the iron environment on substitution of zinc. This result further suggests that in mixed-metal clusters the intrinsic properties of each iron site can be studied without the complexities arising from the exchange coupling.

There is increasing evidence for a new group of binuclear metalloenzymes, the purple acid phosphatases (PAP),[2-12] and much effort has been devoted to their characterization.[13-25] Isolated from mammals[2,4,5] and plants,[6,12] these glycoproteins have a unique active site comprising two interacting metal

(1) (a) University of Illinois. (b) Current address: Physics Department, Northeastern University, Boston, MA 02115. (c) University of Queensland.
(2) Glomset, J.; Porath, J. *Biochim. Biophys. Acta* **1960**, *39*, 1–8.
(3) Jacobs, M. M.; Nyc, J. F.; Brown, D. M. *J. Biol. Chem.* **1971**, *246*, 1419–1425.
(4) Campbell, H. D.; Zerner, B. *Biochem. Biophys. Res. Commun.* **1973**, *54*, 1498–1503.
(5) Schlosnagle, D. C.; Bazer, F. W.; Tsibris, J. C. M.; Roberts, R. M. *J. Biol. Chem.* **1974**, *249*, 7574–7579.
(6) Uehara, K.; Fujimoto, S.; Taniguchi, T. *J. Biochem.* **1974**, *75*, 627–38.
(7) Davis, J. C.; Lin, S. S.; Averill, B. A. *Biochemistry* **1981**, *20*, 4062–4067.
(8) Antanaitis, B. C.; Aisen, P. *Adv. Inorg. Biochem.* **1983**, *5*, 111–136.
(9) Andersson, G.; Ek-Rylander, B.; Hammarstrom, L. *Arch. Biochem. Biophys.* **1984**, *228*, 431–438.
(10) Hara, A.; Savada, H.; Kato, T.; Nakayama, T.; Yamamoto, H.; Matsumoto, Y. *J. Biochem.* **1984**, *95*, 67–74.
(11) Roberts, R. M.; Bazer, F. W. *Bioessays* **1984**, *1*, 8–11. While the pig allantoic fluid purple acid phosphatase has been called uteroferrin, there is little evidence in support of the implied function.
(12) Beck, J. L.; McConachie, L. A.; Summors, A. S.; Arnold, W. M.; de Jersey, J.; Zerner, B. *Biochim. Biophys. Acta* **1986**, *869*, 61–68.
(13) Campbell, H. D.; Dionysius, D. A.; Keough, D. T.; Wilson, B. W.; de Jersey, J.; Zerner, B. *Biochem. Biophys. Res. Commun.* **1978**, *82*, 615–620.
(14) Gaber, B. P.; Sheridan, J. P.; Bazer, F. W.; Roberts, R. M. *J. Biol. Chem.* **1979**, *254*, 8340–8342.
(15) Keough, D. T.; Dionysius, D. A.; de Jersey, J.; Zerner, B. *Biochem. Biophys. Res. Commun.* **1980**, *94*, 600–605.
(16) Keough, D. T.; Beck, J. L.; de Jersey, J.; Zerner, B. *Biochem. Biophys. Res. Commun.* **1982**, *108*, 1643–1648.
(17) Antanaitis, B. C.; Strekas, T.; Aisen, P. *J. Biol. Chem.* **1982**, *257*, 3766–3770.
(18) Antanaitis, B. C.; Aisen, P. *J. Biol. Chem.* **1982**, *257*, 5330–5332.
(19) Davis, J. C.; Averill, B. A. *Proc. Natl. Acad. Sci. U.S.A.* **1982**, *79*, 4623–4627.
(20) Antanaitis, B. C.; Aisen, P.; Lilienthal, H. R. *J. Biol. Chem.* **1983**, *258*, 3166–3172.
(21) Lauffer, R. B.; Antanaitis, B. C.; Aisen, P.; Que, L., Jr. *J. Biol. Chem.* **1983**, *258*, 14212–14218.
(22) Debrunner, P. G.; Hendrich, M. P.; de Jersey, J.; Keough, D. T.; Sage, J. T.; Zerner, B. *Biochim. Biophys. Acta* **1983**, *745*, 103–106.
(23) Beck, J. L.; Keough, D. T.; de Jersey, J.; Zerner, B. *Biochim. Biophys. Acta* **1984**, *791*, 357–363.
(24) Antanaitis, B. A.; Peisach, J.; Mims, W. B.; Aisen, P. *J. Biol. Chem.* **1985**, *260*, 4572–4574.

0002-7863/89/1511-7239$01.50/0